数理解析研究所講究録
933巻 1995年 124-140

Bifurcations in a Generalized Frenkel Kontorova Model.

M. Peyrard
Laboratoire de Physique, Ecole Normale Supérieure de Lyon, 46 Allée d'Italie, 69364 Lyon Cédex 07, France

O. M. Braun
Institute of Physics Ukrainian Academy of Sciences, 46 Science Avenue, Kiev, UA-252022, Ukraine

Abstract

We study the ground state of a generalized Frenkel-Kontorova (FK) model with a transverse degree of freedom. The model describes a lattice of atoms interacting by long-range repulsive forces, which is submitted to a two-dimensional substrate potential periodic in one direction and parabolic or Toda-like in the transverse direction. When the magnitude of the interatomic repulsion increases, the ground state of the model undergoes a series of bifurcations. In particular, the first bifurcation leads to a zig-zag ground state and results in drastic change of system properties including a cusp in the average elastic constant. The existence of the zig-zag state is fundamentally due to the discreteness of the model. For incommensurate cases, the bifurcations can interplay with the Aubry transition from a pinned to a sliding state so that two different effects of discreteness compete to determine the properties of the system.

I. INTRODUCTION

The standard Frenkel-Kontorova (FK) model describes a chain of particles interacting by an harmonic potential and subjected to a sinusoidal on-site potential [1]. Besides its original aim of modeling crystal dislocations, the FK model has many applications in physics such as the description of magnetic domain walls, atoms adsorbed on a crystalline surface or superionic conductors. When the interaction between the atoms is strong enough, a continuum approximation can be used and the model reduces to the integrable Sine-Gordon system. However, except for magnetic systems, the continuum limit is not valid for most physical applications. Discreteness effect may play a fundamental role and modify drastically the properties of the system.

The standard FK model is a 1 space + 1 time dimensional model with one degree of freedom per site. It is too restrictive for some physical applications because it ignores the

transverse displacements of the atoms. A few attempts to generalize the model to $2+1$ dimensions have been made but they lead to complicated models that can only be studied numerically. Recently a generalized FK model has been introduced [2]. It is still a 1+1 dimensional model, but it has *two* degrees of freedom per site corresponding to longitudinal and transverse displacements of the atoms. This generalized FK model has very interesting properties because in this system lattice discreteness can play two different roles which *compete* against each other to determine the properties of the system as discussed below. Although the generalized FK model does not reduce to a known integrable model, because of its $1+1$ dimensional character an integrable system sufficiently close to it could perhaps be found. Moreover the generalized FK model shows interesting mathematical properties, such as a sequence of bifurcations in its ground state, which could deserve the attention of mathematicians. There are many examples where models issued from physics have provided useful starting points for fundamental studies leading to results that the physicists could then use in their analysis of real systems. We hope that the generalized FK model, with its richness, could perhaps become one additional example.

In section II we briefly review some properties of the standard FK model that are necessary to understand the properties of the generalized model. Section III introduces the generalized FK model and its ground state which shows a sequence of bifurcations when one model parameter is changed. Section IV shows how two different effects of the discrete nature of the model can compete to determine the properties of the system, and section V discusses some extensions and applications to physics.

II. THE STANDARD FK MODEL.

In order to understand the properties of the standard FK model, it is convenient to have in mind the case of a chain of atoms adsorbed on a crystal surface (Figure. 1). The hamiltonian of the system is

$$H = \sum_n \frac{1}{2} m \dot{x}_n^2 + V(x_{n+1} - x_n) + V_s(x_n) \tag{1}$$

If it were alone, the coupling potential $V(x_{n+1} - x_n)$ would impose an interatomic distance a_A. The substrate potential $V_s(x_n)$ has a period a_s. Let us consider for instance the case $V(x_{n+1} - x_n) = \frac{1}{2}(x_{n+1} - x_n - a_A)^2$ and $V_s(x_n) = \frac{1}{2}\epsilon[1 - \cos(2\pi x_n/a_s)]$ which reduces to the integrable sine-Gordon model in the continuum limit. The ground state of the system is obtained by minimizing the potential energy of the system. In terms of ϕ_n defined by $x_n = na_s + \phi_n$ which measures the position of the n^{th} atom with respect to the n^{th} minimum of the substrate potential, the minimization of the potential energy leads to

$$(\phi_{n+1} + \phi_{n-1} - 2\phi_n) - \epsilon \sin\left(\frac{2\pi}{a_s}\phi_n\right) = 0\,. \tag{2}$$

In the continuum limit, valid in the strong coupling case when the coupling potential is much larger than the substrate potential, this equation is well approximated by the sine-Gordon equation.

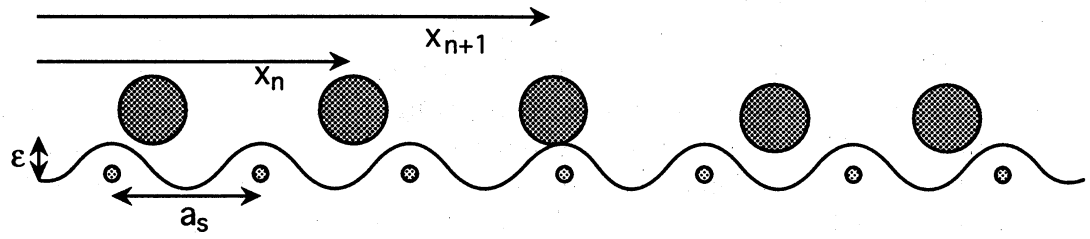

FIG. 1. A physical system described by the standard FK model: atoms on a crystal surface. The model describes a one dimensional chain of atoms interacting through a potential v, adsorbed on a crystal surface that generates a substrate potential of period a_s. Only longitudinal displacements of the atoms parallel to the surface are considered. The positions of the atoms are given by their distance x_n with respect to an origin O.

When the two distances a_A and a_s are commensurate, i.e. have a rational ratio, the ground state of the system is simple because it is periodic. The case of incommensurate a_A/a_s is more interesting. In this case discreteness plays a crucial role and is responsible for a transition, known as the Aubry transition [3,4], between two states of the system which have completely different properties. In order to understand the origin of this transition, it is convenient to replace Eq. (2) by a discrete mapping by defining $p_n = \phi_n - \phi_{n-1}$. It becomes

$$\begin{pmatrix} p_{n+1} \\ \phi_{n+1} \end{pmatrix} = \begin{pmatrix} p_n + \epsilon \sin\left(\frac{2\pi}{a_s}\phi_n\right) \\ p_n + \phi_n + \epsilon \sin\left(\frac{2\pi}{a_s}\phi_n\right) \end{pmatrix}, \tag{3}$$

which is known as the "standard map". In the limit $\epsilon \to 0$, where the coupling interaction dominates, the standard map is in a non-chaotic domain. A diagram of ϕ_{n+1} versus ϕ_n (for varying n) shows a smooth closed curve (torus in the reduced phase space). In this case, ϕ takes all the values in the range $[0, a_s]$, indicating that there are atoms on tops of the substrate potential maxima as well as in the minima, as schematized on fig. 2-a. Therefore the atomic chain is totally free to slide with respect to the substrate because it costs the system no energy: some atoms go down the substrate potential maxima while others go up [3,4]. This is why this strong-coupling state of the FK model is called the sliding phase. If, on the contrary the substrate potential is large with respect to the interatomic coupling, the atoms tend to fall into the minima of the substrate while the maxima are never occupied as shown on the lower part of fig. 2-a. The torus of the diagram ϕ_{n+1} versus ϕ_n is broken into isolated islands and the atomic chain is now pinned to the substrate (hence the name "pinned phase") because its translation requires bringing atoms on the maxima of the substrate potential which costs energy. The difference between the sliding and the pinned state can also be detected in the spectrum of the small amplitude excitations of the ground state. In the sliding case the frequencies start at $\omega = 0$, which corresponds to the translational mode of the system, while in the pinned phase the spectrum has a gap and starts above a finite value ω_b [4]. The transition from the sliding to the pinned state

occurs for a well defined value of $\epsilon = \epsilon_c$ which corresponds to the appearance of chaos in the standard map.

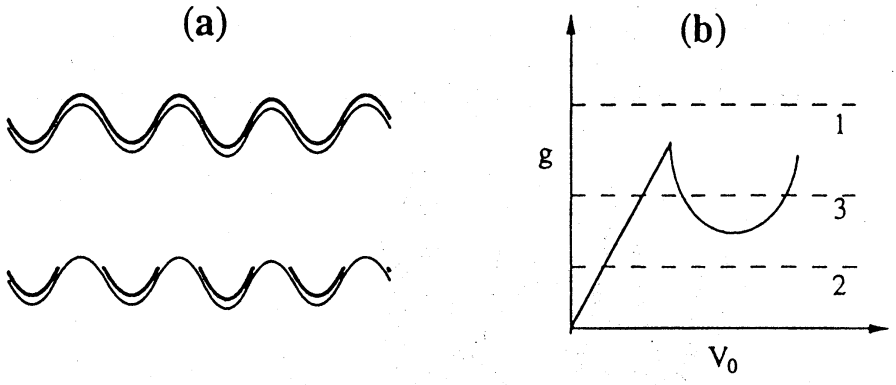

FIG. 2. (a) Schematic picture of the positions of the atoms with respect to the substrate potential on the two sides of the Aubry transition. The heavy line shows the occupied regions of the potential. In the weak coupling domain (top figure), the top part of the maxima are not occupied. In the strong coupling domain (lower figure), all regions, including the top of the barriers, are occupied. (b) Schematic figure illustrating the possible competition between the zig-zag and Aubry transitions (see Sec. IV). The three horizontal lines correspond to three possible positions of g_{Aubry} with respect to the cusp in elastic constant due to the transition to a zig-zag state.

III. GROUND STATE OF THE GENERALIZED FK MODEL.

A. Model

In addition to the atomic displacements parallel to the crystal surface, the generalized FK model considers also their displacements along the direction y orthogonal to the surface. The substrate potential, now written $V_s(\mathbf{r})$ with $\mathbf{r} \equiv (x, y)$, includes an additional term, depending on y which describes the confinement of the atoms in the vicinity of the surface. We assume that $V_s(\mathbf{r})$ is the sum of two terms,

$$V_s(\mathbf{r}) = V_x(x) + V_y(y), \tag{4}$$

where $V_x(x)$ is a periodic potential along the chain which is assumed to be sinusoidal as in the standard FK model,

$$V_x(x) = \frac{1}{2}\epsilon_s[1 - \cos(2\pi x/a_s)], \tag{5}$$

and $V_y(y)$ is the confining potential in the transverse direction.

Two cases will be considered, a symmetric (even) potential $V_y(y)$ which is taken to be parabolic,

$$V_y(y) = \frac{1}{2}m_a\omega_{0y}^2 y^2 \,, \tag{6}$$

where ω_{0y} is the frequency of a single-atom vibration in the transverse direction and m_a the atomic mass, and a non-symmetric anharmonic potential which has been chosen with a Toda-like form

$$V_y(y) = \omega_{0y}^2 y_{anh}^2 \left[\exp(-y/y_{anh}) + (y/y_{anh}) - 1\right] . \tag{7}$$

Figure 3 shows the shape of the substrate potential for a symmetric $V_y(y)$ potential.

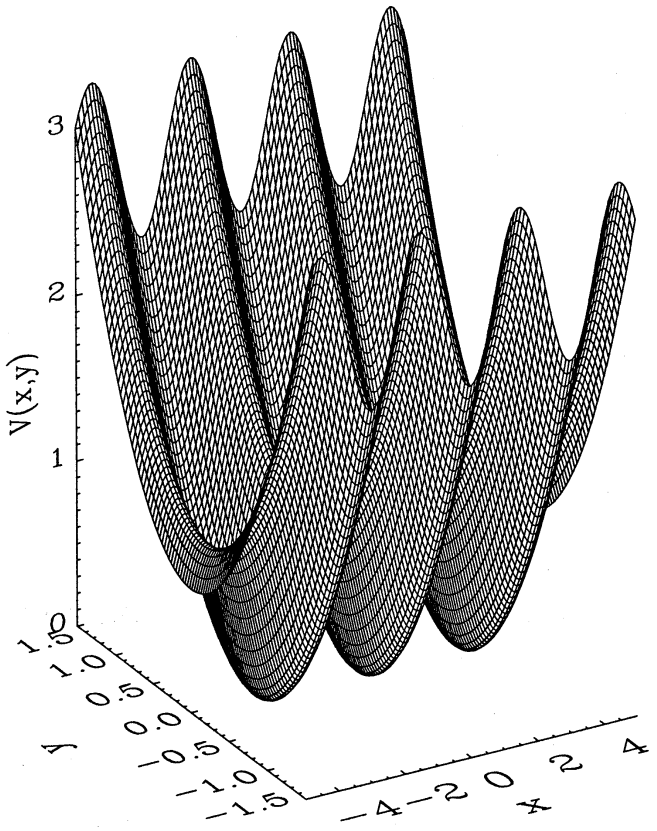

FIG. 3. The two-dimensional substrate potential of the generalized FK model for a symmetric confining potential $V_y(y)$.

It is convenient to use units such that the atomic mass is $m_a = 1$, the amplitude of the periodic substrate potential is $\epsilon_s = 2$ and its period is $a_s = 2\pi$, so that the frequency of longitudinal vibrations $\omega_{0x} = (\epsilon_s/2m_a)^{\frac{1}{2}}(2\pi/a_s)$ is equal to 1.

For noninteracting atoms, the x and y degrees of freedom are decoupled due to the simple form chosen for the substrate potential in Eq.(4). However the interatomic interaction couples them. As long as the atoms use only an attractive branch of the interaction potential, the static properties of the model are equivalent to those of the standard FK model (but the dynamics is modified). In a number of physical systems, however, the interatomic interaction is repulsive or has at least a repulsive branch. It can be due to Coulomb repulsion between ions in superionic conductors or between protons in hydrogen-bonded molecules,

or to Coulomb or dipole-dipole repulsion of atoms adsorbed on semiconductor or metal surfaces. We consider here the case of a Coulomb repulsion between the atoms

$$V(r) = V_0/r, \tag{8}$$

where V_0 characterizes the amplitude of repulsion. Note that qualitative results do not depend on the specific form of $V(r)$ provided that the repulsion is concave, i.e. if $V(r)$ decreases monotonically with increasing distance r between the atoms. Consequently, in attempts to find an integrable model close to the generalized FK model, the exact form of the repulsive interaction could be changed. Since the Coulomb repulsion is a long range interaction, the interatomic interaction is not restricted to nearest neighbors, as in the standard FK model, but extended to all atoms in the lattice.

For repulsive interactions the boundary conditions are essential to determine the properties of the system because, with free boundaries, the chain of atoms would tend to decrease its energy by expanding indefinitely. In a physical system, this is generally not possible and for instance for atoms adsorbed on a surface, the average density of atoms is imposed by the experimental conditions. We represent this situation by imposing a fixed density of atoms. The chain consists of N atoms distributed on the length $L = Ma_s = Na_A$, where M is the number of minima of $V_x(x)$ and a_A is the mean interatomic distance along the chain. Therefore the system is characterized by the dimensionless concentration $\theta = N/M = a_s/a_A$ which is kept fixed in the limit $N, M \to \infty$. The density of atoms is constrained by using periodic boundary conditions with a period which is a multiple of $Na_A = Ma_s$. The total potential energy of the system is

$$U = \sum_{i=1}^{N} \left[V_s(\mathbf{r}_i) + \frac{1}{2} \sum_{i'=1}^{N^*} [V(|\, \mathbf{r}_i - \mathbf{r}_{i+i'} \,|) + V(|\, \mathbf{r}_i - \mathbf{r}_{i-i'} \,|)] \right], \tag{9}$$

where the index i labels the atoms, and the limit $N, N^* \to \infty$ is assumed. The ground state configuration corresponds to the absolute minimum of U. So to find the atomic coordinates in the ground state $\{\mathbf{r}_i^{(0)}\} \equiv \{x_i^{(0)}, y_i^{(0)}\}$, we look for static configurations by solving the set of equations $\partial U/\partial x_i = 0$, $\partial U/\partial y_i = 0$, $i = 1, \cdots, N$, and then select the ground state configuration which gives the absolute minimum of U.

When the ground state coordinates are known, we can perform a linear stability analysis by expanding linearly the equations of motion of the atomic chain and looking for the eigenfrequencies of the dynamical matrix. For commensurate cases (θ rational), the ground state configuration is periodic and it is convenient to take the Fourier transform of the equations of motion which defines the frequencies $\omega_j(k)$ as a function of a wavevector k belonging to the first Brillouin zone of the periodic lattice.

For a stable configuration all eigenfrequencies must be positive. When, for some model parameters, one of the frequencies vanishes, $\omega_j(k^*) = 0$, the corresponding configuration becomes unstable and evolves into a new configuration with the period $a^* = \pi/k^*$. The eigenvector associated to the vanishing frequency determines the structure of the new ground state. This scenario corresponds to a continuous (second-order) phase transition. Moreover the model may also exhibit discontinuous (first-order) phase transitions when a model parameter (e.g., V_0) is changed. They occur when the energy of a metastable configuration becomes equal to the energy of the ground state configuration at a transition point

$V_0 = V_{bif}^{(m)}$, and beyond this point the metastable and ground state configurations are exchanged.

As discussed in Sect. II, for the standard FK model, the average coupling energy is important because, for a given substrate in the incommensurate case, it determines whether the system is in a sliding or in a pinned phase. As the existence of the Aubry transition can be deduced from very general arguments comparing the coupling and the on-site potential energies, we can expect it to occur in the generalized FK model too. Therefore it is useful to calculate for each state the average elastic constant g defined by

$$g = \frac{1}{N}\sum_{i=1}^{N} g_i \,, \tag{10}$$

with

$$g_i = \frac{1}{2}\sum_{i'=1}^{N^*}\left[\frac{\partial^2}{\partial x_i^2}\left(V(|\,\mathbf{r}_i - \mathbf{r}_{i+i'}\,|) + V(|\,\mathbf{r}_i - \mathbf{r}_{i-i'}\,|)\right)\right]_{all\ \mathbf{u}=0} . \tag{11}$$

For the standard FK model g defined by eqs. (10) and (11) coincides with the dimensionless coupling constant $(a_s^2/2\pi^2\epsilon)V''(a_s)$.

Most of the results of the present work have been obtained from a numerical analysis. The ground state is obtained by a minimization of the potential energy of the system by a relaxation procedure similar to the simulated annealing method to avoid the convergence toward secondary minima [5]. In numerical calculations we can only take into account a finite number N^* of interacting neighbors. These neighbors cannot be simply chosen at the starting of the calculation because, with transverse motions allowed, the sequence of the atoms can change. Therefore we have to use a standard procedure of molecular dynamics, i.e. select a cutoff distance L^* ($L^* \gg a_A$) and include in the calculation only the atoms which are such that $r_{ii'} \leq L^*$.

In order to select the configuration with the lowest energy, we calculate the potential energy per atom, E. Unfortunately, for the Coulomb interatomic repulsion the total energy of interaction depends on the cutoff distance L^*, and diverges as $\ln L^*$ in the limit $L^* \to \infty$. To avoid this problem, we subtract from the total potential energy a constant equal to the repulsion energy in the uniform configuration with the atomic coordinates $x_i = ia_A$, $y_i = 0$. Thus, each configuration is characterized by an energy

$$E = \frac{1}{N}\sum_{i=1}^{N}\left[V_s(\mathbf{r}_i^{(0)}) + \frac{1}{2}\sum_{i'=1}^{r_{i,i+i'}<L^*} V(r_{i,i+i'}) + \frac{1}{2}\sum_{i'=1}^{r_{i,i-i'}<L^*} V(r_{i,i-i'})\right] - S(N_m)V_0/a_A, \tag{12}$$

where $S(N_m) = 1 + \frac{1}{2} + \frac{1}{3} + \cdots + \frac{1}{N_m}$ and $N_m = \mathrm{int}(L^*/a_A)$.

B. The first bifurcation in commensurate states.

In the case of the standard FK model, for commensurate cases the ground state is almost trivial because it is periodic and can be obtained by solving a finite set of coupled nonlinear equations. For the generalized FK model, even for a commensurate case, the

situation is more interesting because, when V_0 reaches some critical value V_{bif}, the ground state bifurcates from a state in which all the atoms are aligned with $y_n = 0$ to a zig-zag state where atoms with positive and negative $y_n \neq 0$ alternate. An example is shown on fig. 4-a. It should be noticed that this bifurcation is an *intrinsically discrete property* of the model. In a continuous model one cannot define such a zig-zag configuration.

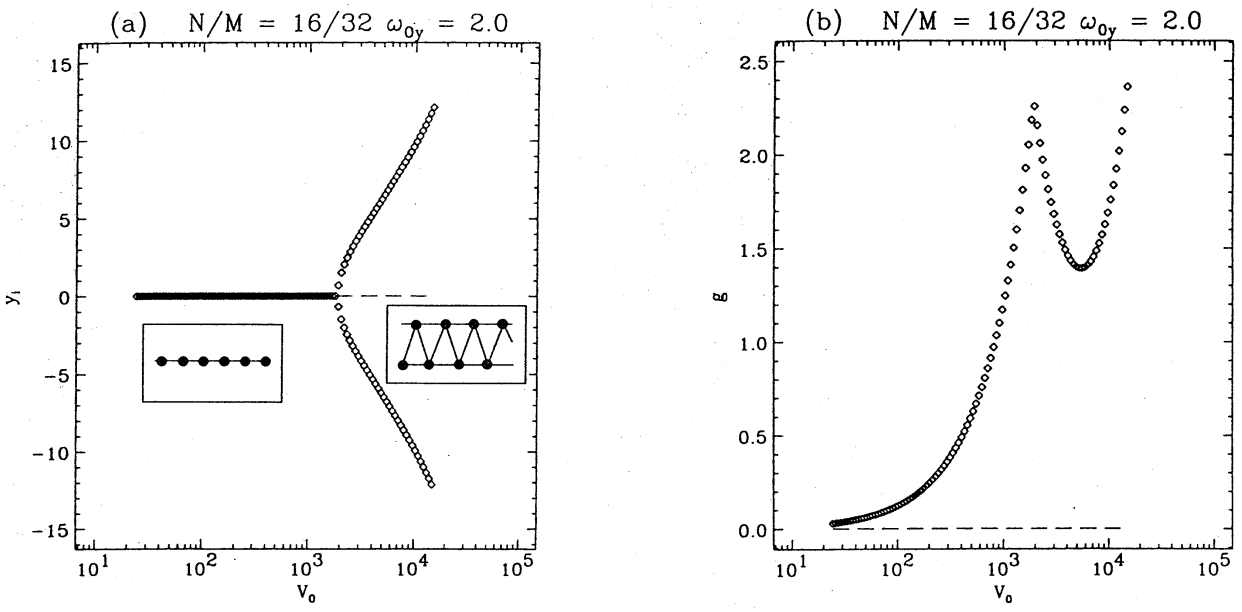

FIG. 4. Example of bifurcation of the ground state of the generalized FK model in a commensurate case, $\theta = N/M = 16/32$. Fig. (a) shows the transverse displacements y of the atoms as a function of the amplitude V_0 of the interaction potential. The inserts show schematically the atomic positions on both sides of the bifurcation. Fig. (b) shows the average elastic constant g as a function of V_0 for the same system.

Although the exact ground state configuration can only be obtained numerically for a general commensurate state, in the simplest case of the commensurate concentration $\theta = N/M = a_s/a_A = 1/q$ with an integer q such that the average interatomic distance a_A is a multiple of the lattice constant a_s, $(a_A = qa_s)$, an analytical determination of the bifurcation point is easy to obtain from the linear stability analysis. In this case, for a small interatomic repulsion, the ground state is trivial (TGS), and all atoms are situated at the bottoms of the corresponding wells, $x_i^{(0)} = ia_A$ and $y_i^{(0)} = 0$. The elementary cell of the system contains one atom only, and the phonon spectrum consists of two branches (see fig. 5-a). The first branch corresponds to motion along the x direction,

$$\omega_1^2(k) = \omega_{0x}^2 + 2\sum_{l=1}^{\infty} V''(la_A)[1 - \cos(kla_A)], \tag{13}$$

and the second branch to motion along the y direction,

$$\omega_2^2(k) = \omega_{0y}^2 + 2\sum_{l=1}^{\infty}[V'(la_A)/(la_A)][1 - \cos(kla_A)], \tag{14}$$

where $\mid k \mid \leq 1/2q$. Notice that the motions along the x and y directions are decoupled.

For repulsive interatomic interactions, $V'(la_A) < 0$ so that, when the magnitude of the interatomic interaction increases, the frequency $\omega_2(k)$ decreases and reaches zero at some critical value $V_0 = V_{bif}$. If the interatomic repulsion decreases monotonically with increasing r (i.e. if V' is always negative), the first instability arises at the momentum $k = \pm 1/2q$. The corresponding bifurcation value V_{bif} can be determined from the equation

$$\omega_{0y}^2 + 4\sum_{p=0}^{\infty} \frac{V'[(2p+1)a_A]}{(2p+1)a_A} = 0. \tag{15}$$

In particular, for the Coulomb repulsion (8) V_{bif} is equal to

$$V_{bif} = \omega_{0y}^2 a_A^3/4C, \tag{16}$$

where $C \equiv \sum_{p=0}^{\infty}(2p+1)^{-3} = 1.05179\cdots$

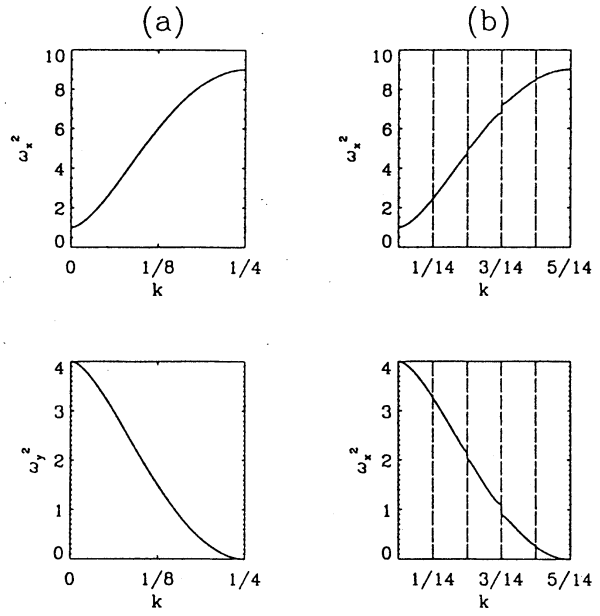

FIG. 5. Phonon spectrum of the commensurate trivial ground state for $\omega_{0y} = 2$ at $V_0 = V_{bif}$. (a) $\theta = 1/2$ ($N^* = 64$), $V_{bif} = 1886$ and (b) $\theta = 5/7$ ($N^* = 60$) $V_{bif} = 644.7$. In the case (b) we use the scheme of extended Brillouin zones.

Thus, for any monotonically decreasing interatomic repulsion the first bifurcation leads always to a continuous transition from the trivial ground state to the zigzag-ground state with atomic coordinates $x_i^{(0)} = ia_A$, $y_i^{(0)} = (-1)^i b$. The amplitude b of the transverse atomic shifts is determined by the equation

$$\omega_{0y}^2 + 4\sum_{l=0}^{\infty} V'(r_l)/r_l = 0, \quad r_l = [4b^2 + a_A^2(1+2l)^2]^{1/2}. \tag{17}$$

In the ZGS the value of the transverse splitting b increases with V_0 as is shown in fig. 4-a.

It will be convenient to use henceforth a dimensionless amplitude of interatomic repulsion defined as $v = d/a_A$, where $d = (4b^2 + a_A^2)^{1/2}$ is the distance between the nearest neighbors in the ZGS, so that $v_{bif} = 1$.

To obtain analytical estimates, let us consider the case of a Coulomb repulsion restricted to nearest and next nearest neighbors only. In this case the interaction is limited inside one cell of the ZGS so that only $p = 0$ has to be considered in eqs. (15-17), and we get

$$V_{bif} = \frac{1}{4}\omega_{0y}^2 a_A^3, \tag{18}$$

$$b = \frac{1}{2}\left[\left(4V_0/\omega_{0y}^2\right)^{2/3} - a_A^2\right]^{1/2}, \tag{19}$$

$$d = \left(4V_0/\omega_{0y}^2\right)^{1/3}, \tag{20}$$

and

$$v = \left(4V_0/\omega_{0y}^2 a_A^3\right)^{1/3}. \tag{21}$$

The average elastic constant (10) for the TGS is equal to

$$g_{(TGS)} = \frac{9}{4}\frac{V_0}{a_A^3}, \tag{22}$$

while for the ZGS it is determined by the expression

$$g_{(ZGS)} = \frac{1}{16}\omega_{0y}^2\left(v^3 + 12/v^2 - 4\right). \tag{23}$$

According to Eqs.(22) and (23), the elastic constant g for the TGS increases linearly with V_0 up to the value $g_{bif} = 9\omega_{0y}^2/16$. But after the bifurcation g decreases, reaches the local minimum $g_{min} = 4.705\omega_{0y}^2/16 \sim 0.5\, g_{bif}$ at $v = 8^{1/5}$, and then rises again.

Figure 4-b shows the numerical results for $\theta = \frac{1}{2}$ and $\omega_{0y} = 2$ ($N = 16$, $M = 32$), taking into account the interaction of a large number of neighbors ($N^* = 64$). The results are in agreement with the predictions of the simple approach described above. Note that the cusp of the elastic constant g at the bifurcation point V_{bif} explains many remarkable properties of the model, as discussed in Sect. III.

The properties of the system with a complex, but commensurate, elementary cell are similar to the properties found above for a simple unit cell with only one atom. Let us consider a rational atomic concentration $\theta = s/q$, where s and q are relatively prime integers, and $s < q$ so that there is not more than one atom in one well of the longitudinal substrate potential. The ground state of the system is still periodic, with period $sa_A = qa_s$, and for V_0 below the bifurcation point, the ground state is again a trivial ground state with $y = 0$ for all atoms. Their x positions along the chain are now shifted from the minima of the potential wells and these shifts increase with V_0. The elementary cell of the TGS consists now of s atoms. Therefore, the phonon spectrum has to have $2s$ branches as shown in fig. 5-b where for clarity we use the scheme of extended Brillouin zones so that the momentum k varies in the range $\mid k \mid \leq k_\theta$, $k_\theta = sk_B = \theta/2$ with $k_B = \pi/sa_A = 1/2q$ being the boundary of the first Brillouin zone in our units where $a_s = 2\pi$. Fig. 5-b shows that the first instability arises again at $k = \pm k_\theta$, and it corresponds to a continuous transition from the TGS to the ZGS. The ZGS has the period $2sa_A$.

C. Higher-order bifurcations.

Taking into account long range forces and not only nearest neighbor interactions, allows further bifurcations beyond the first instability leading to the ZGS.

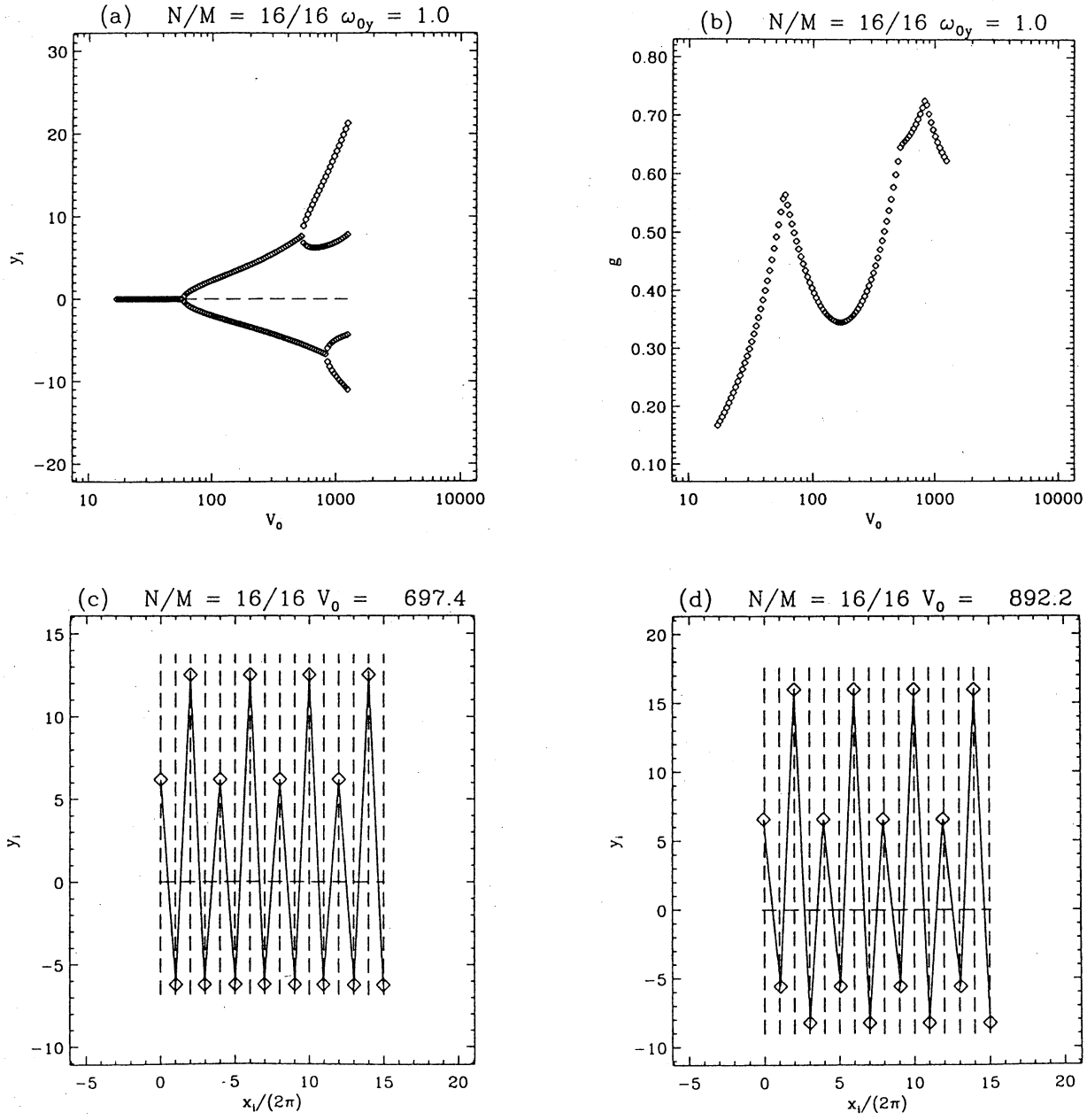

FIG. 6. Transverse atomic displacements (a) and elastic constant g versus V_0 (b), and two typical configurations for $V_0 = 697$ (c) and $V_0 = 892$ (d) for the Toda transverse substrate potential. $\theta = 1$ ($N = M = 16$ and $N^* = 64$), $\omega_{0y} = 1$, $y_{anh} = 20$.

The simplest situation is observed for a non symmetric confining potential $V_y(y)$ such as the Toda potential of Eq. (7). Figure 6 shows one example for the simplest commensurate situation $\theta = 1$. Three bifurcations can be observed. Each new bifurcation induces a cusp in the average elastic constant as shown on fig. 6-b. After the first bifurcation the positive and negative transverse displacements of the atoms are not the same, in agreement with the asymmetry of the potential, i.e. the resulting zig-zag ground state is no longer symmetric with respect to $y = 0$. It is easy to get a qualitative understanding of the second bifurcations by viewing the zig-zag ground state as a combination of two "sub-chains", the upper sub-chains corresponding to atoms having a positive displacements and the down sub-chain to atoms having a negative displacement. Since the interactions are not restricted to first neighbors, atoms in a sub-chain interact with each other in a similar manner as the atoms in the original chain. One can mentally isolate one of the sub-chains, the role of the second one being simply to create a local minimum around the y value of the sub-chain that we chose to study. It is then possible to consider the linear stability of the chosen sub-chain. The analysis is very similar to that of the total chain if we include the effect of the second sub-chain, assumed to stay fixed, as an external potential, and we again find that the sub-chain tends to bifurcate into a "sub-zig-zag" configuration. Such a configuration can be observed on fig. 6-c. For a higher value of V_0 the down sub-chain becomes unstable too and bifurcates in a sub-zig-zag structure as shown on fig. 6-d.

The bifurcation points are determined by the curvature of $V_y(y)$ for y equal to atomic coordinates in one sub-chain. To find the bifurcation points, we can deduce, similarly to Eq.(18), an equation

$$V_{bif}^{(m)} = \frac{1}{4}(\omega_{eff}^{(m)})^2(2^{m-1}a_A)^3 \,, \tag{24}$$

where we have introduced $\omega_{eff}^2 = \left[\frac{\partial^2}{\partial y^2}V_{sub}(r)\right]_{r=r_i}$ instead of ω_{0y}^2. Because $\omega_{eff}^2 = \omega_{0y}^2 \exp(-\beta y)$ for the Toda potential (7), we see that the upper and down sub-chains are now characterized by different effective frequencies ω_{eff}^{up} and ω_{eff}^{down} such that $\omega_{eff}^{up} < \omega_{0y} < \omega_{eff}^{down}$. So the instability arises first at $V_0 = V_{bif}^{(up)}$ in the upper sub-chain, and it leads to creation of a subzigzag ground state configuration in the upper sub-chain only (fig. 6-c). Then, at $V_0 = V_{bif}^{(down)} > V_{bif}^{(up)}$, the down sub-chain becomes unstable, creating a subzigzag configuration in the down-sub-chain too (fig 6-d). Thus, the second bifurcation leads to splitting of the two-sub-chain structure into a three-sub-chain configuration, then into a four-sub-chain configuration. We could thus expect that the evolution of the ground state configuration would proceed in an analogous manner: additional bifurcations could start on the top sub-chain leading to the creation of the next sub-zigzag structure (i.e., the next splitting of the top sub-chain), and then this splitting would spread sequentially to sub-chains with smaller y values. This scenario reminds of the well-known Feigenbaum picture for the transition from a regular to the chaotic behavior, so it should end at some accumulation point by the creation of an incommensurate structure for a rational θ.

The picture discussed above is however oversimplified because the distance between the central sub-chains (i.e. the sub-chains with the smallest transversal displacements) does not increase fast enough, and the interaction between them increases with V_0. Therefore they cannot be treated as independent. The high order bifurcations predicted by this discussion

are very difficult to observe numerically, and, as shown in fig. 6 we have seen only 3 bifurcations (leading to the splitting of the system into 4 sub-chains) in our calculations.

The case of a symmetric confining potential $V_y(y)$, which may seem simpler because of the additional symmetry, turns out to be more complicated, because the top and down sub-chains become unstable for the same value of the repulsive interaction V_0. Since a system close to an instability is very sensitive to small perturbations, the instability of each sub-chain affects the other. A separate study of one sub-chain can no longer lead to useful results and the study of the full system is required. An analytical linear stability analysis is however possible in the simple case $\theta = 1$ if we consider only nearest and next nearest neighbor interactions [5]. Because the zigzag configuration for $\theta = 1$ has two atoms in the elementary cell, the phonon spectrum consists of four branches $\omega_j(k)$, j=1 to 4. Contrary to the case of the TGS, in the ZGS x and y modes are coupled. In order to find an instability point v_{crit}, we have to take the lowest root $\omega_{min}(k) = \min_j \omega_j(k)$ and then look for the point where $\omega_{min}(k)$ reaches zero for the first time at some $k = k^*$. The analysis of the spectrum shows that the instability of the zig-zag configuration occurs through a first order transition in which a state which was metastable becomes the minimum energy configuration. Thus, beginning from the ZGS, the ground state of the system undergoes a series of first-order transitions with increasing interatomic repulsion.

These predictions are based on analytical expressions in the case $\theta = 1$ with only nearest and next nearest interactions. They should be checked by numerical calculations. However the calculations become very difficult because, for complicated structures, it is very difficult to make sure that we have obtained the true ground state after relaxation. Therefore we have limited our investigations to a few particular situations without attempting an exhaustive study which would have been of limited physical interest because the perfectly symmetric potential is an idealized case.

IV. AUBRY TRANSITIONS

As mentioned above, since the Aubry transition of the standard FK model can be deduced from general arguments on the competition between the on-site potential and the interatomic coupling, one can expect to find it in the generalized FK model too. The question which arises naturally is to what extent the introduction of a transverse degree of freedom in our model can affect the Aubry transition. The answer can be derived from the variation of the elastic constant g versus V_0 obtained in the previous section. Because the bifurcation point V_{bif} is determined by the curvature of the transverse substrate potential, $V_{bif} \propto \omega_{0y}^2$ according to Eq.(18) while the Aubry transition concerns essentially the longitudinal displacements, the relative positions of the two transitions can change depending on model parameters. Depending on the value of ω_{0y}^2, we can predict three different scenario for the behavior of the system with increasing V_0 as shown schematically on fig. 2-b.

(a) The case of ω_{0y} below a first threshold ω^*, $\omega_{0y} < \omega^*$, such that $V_{bif} < V_{Aubry}$ (case 1 on fig.2). In this case the Aubry transition will not occur because the first bifurcation, to a zig-zag state, which reduces the effective interatomic coupling, occurs before g can reach the magnitude g_{Aubry} required for the Aubry transition. Taking $g_{Aubry} \simeq 1$ for the golden mean $\theta_{g.m.}$ and $g_{bif} \simeq 9\omega_{0y}^2/16$, the value ω^* can be estimated as $\omega^* \approx 4/3$.

(b) The case of large ω_{0y}, $\omega_{0y} > \omega^{**}$ (where ω^{**} is a second characteristic value) , for which $V_{bif} \gg V_{Aubry}$ and $g_{Aubry} < g_{min} \equiv \min g(V_0)$ for all V_0 within the ZGS (case 2 on figure 2). In this case the Aubry transition is observed when V_0 reaches V_{Aubry} and the bifurcation which occurs later does not bring any qualitative change in the system behavior because the minimum of g after the bifurcation is above g_{Aubry}. Only a higher order bifurcation could bring a qualitative change. Taking $g_{min} \simeq 0.5\, g_{bif}$, the value ω^{**} can be estimated as $\omega^{**} \approx 4\sqrt{2}/3 \approx 1.9$ for $\theta = \theta_{g.m.}$.

(c) For intermediate ω_{0y}, $\omega^* < \omega_{0y} < \omega^{**}$ (case 3 on fig. 2), when V_0 is increased, the system undergoes first an Aubry transition in which the pinned ground state is transformed to a sliding ground state. But then the bifurcation to a zig-zag state can reduce the average elastic constant below g_{Aubry}. The system undergoes a *reverse* Aubry transition and the lattice gets pinned to the substrate again. The further increase of g which occurs after the minimum can cause again a direct Aubry transition restoring the sliding state, at least up to the second bifurcation.

In order to check numerically these predictions, we should in principle chose N/M irrational, which is not possible for a finite system because M and N must be integers in our calculations. There are however sequences of rational numbers which approach closely an irrational number. They can be obtained from the continuous fraction expansion of the irrational number. An example is provided by the Fibbonacci sequence

$$1 \to \frac{2}{3} \to \frac{3}{4} \to \frac{5}{7} \to \frac{8}{11} \to \frac{13}{18} \to \frac{21}{29} \to \frac{34}{47} \to \cdots, \tag{25}$$

which tends to $\theta'_{g.m.} = (3+\sqrt{5})/(5+\sqrt{5})$, equivalent to the golden mean for the Aubry transition. We chose $N = 34$, $M = 47$, and $N^* = 34$ in our study. Note, however, that in a numerical simulation the value θ is always rational, so the ground state will stay slightly pinned.

To simulate the intermediate case (c), which corresponds to the most interesting situation, we take $\omega_{0y} = 1.5$ which is in the range estimated above, $4/3 < \omega_{0y} < 4\sqrt{2}/3$. The results are presented in fig. 7. The Aubry transition takes place before the bifurcation, and then g continues to rise to the value $g_{bif} = 1.189$ (see fig. 7-b). But after the bifurcation which takes place at $V_{bif} = 381$, the elastic constant g decreases and reaches the minimum $g_{min} = 0.771$ which is lower than g_{Aubry} at $V_0 = 1079$. Figure 7 shows that, in the vicinity of the minimum of the function $g(V_0)$, the atomic displacements decrease strongly and there is not any more an atom on top of the maxima of $V_x(x)$, as expected (see fig. 2-a). Thus, in the region near the minimum of $g(V_0)$ the ground state seems again pinned. A sensitive test of the existence of the Aubry transitions is provided by the calculation of the linear response of the atomic chain to an external force F applied to all the atoms, along the direction of the x axis. We calculate the mean shift of the atoms, $\Delta x_{shift} = (1/N)\sum_{i=1}^{N}(x_i - x_i^{(0)})$, with respect to their positions without the force, $x_i^{(0)}$, and define a susceptibility as

$$\chi = \Delta x_{shift}/F. \tag{26}$$

We expect $\chi \to \omega_{0x}^{-2}$ in the limit $V_0 \to 0$, and $\chi \to \infty$ in the sliding state. The behavior of the susceptibility (fig. 7-c) attests that we have observed the predicted reverse Aubry transition from the sliding to the pinned state at $V_0 = 578$ when $g = 0.898$. With further increase of V_0, after reaching the minimum the elastic constant increases again, and at $V_0 = 879$

when $g = 782$ the system undergoes a second direct Aubry transition before the second bifurcation.

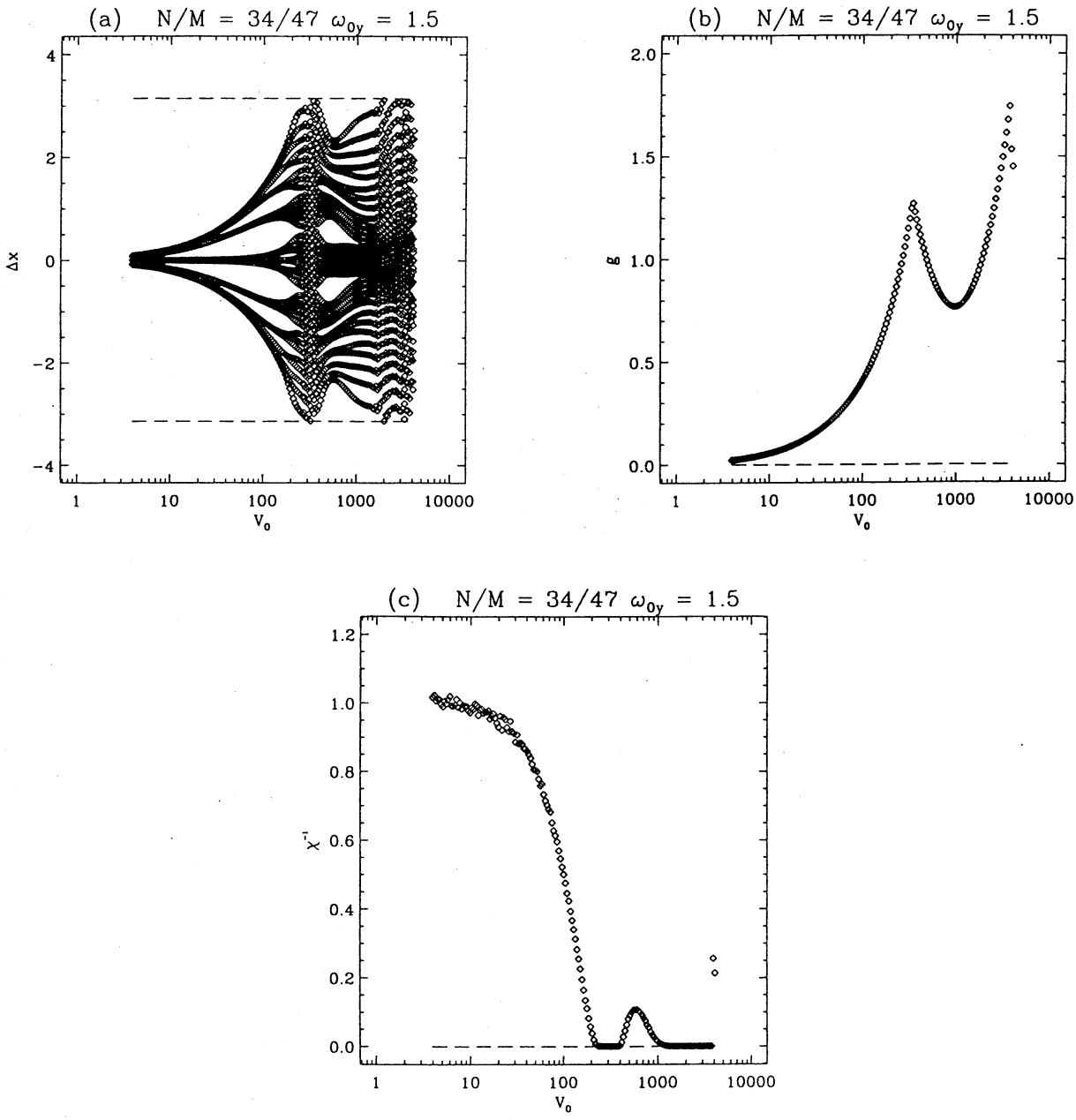

FIG. 7. (a) Longitudinal displacements Δx of the atoms with respect to the nearest minimum of $V_x(x)$, (b) transverse displacements y, (c) inverse susceptibility χ^{-1} versus V_0 for the incommensurate structure ($\theta = 34/47$, $N^* = 34$) for $\omega_{0y} = 1.5$. The inverse susceptibility shows the existence of a reverse Aubry transition followed again by a direct transition for which χ^{-1} drops again to 0.

V. CONCLUSION

The generalized FK model, in which a transverse degree of freedom has been added to the usual longitudinal motions, is an interesting example of a nonlinear lattice with more than one degree of freedom per unit cell. From the mathematical point of view, very little is known for such systems, particularly when discreteness is important. The properties of the generalized FK model show however that they deserve interest, in spite of the analytical difficulties, for two reasons. First the model exhibits a very rich behavior even when one considers only the static properties of the ground state. We found for instance a sequence of bifurcations that could perhaps lead to a chaotic (glass-like) spatial structure of the ground state while, for the standard FK model, if chaotic states can exist in the discrete case, they never correspond to the ground state of the system. The richer behavior of the generalized FK model arises from the coupling of several instabilities (the instabilities of the different sub-chains). The generalized FK shows also an example where discreteness is crucial (we would not have a zig-zag state without discreteness) and can play several competitive roles to determine the structure of incommensurate systems. Moreover the dynamics of the commesurate generalized FK model exhibits interesting features such as different types of soliton-like excitations in the zig-zag state [2]. The second reason for the interest of the generalized FK model lies in its various applications in physics, in particular to describe atoms adsorbed on surfaces, epitaxial crystal growth and surface diffusion [6]. The model can for instance reproduce the reconstruction of the first layer, observed in some cases of epitaxial growth, when the second layer begins to grow [6]. It can also explain some observations of anomalously fast diffusion of atoms on surfaces by showing how some extra atoms added to a filled first layer can generate metastable defects which are extremely mobile [6].

Although the generalized FK model is significantly more complicated than the standard FK model because it has been built with complex physical applications in mind, it is still tractable due to its one-dimensional character which allows analytical studies in some particular cases. From a mathematical point of view, it would be worthwhile to look for the simplest model that would preserve the main features of the generalized FK model discussed here while allowing more complete theoretical studies.

ACKNOWLEDGMENTS

M.P. would like to thank S. Takeno and S. Homma for the opportunity of a long term visit in Japan which made possible his participation in this conference.

This work was supported in part by the NATO Linkage Grant LG 930236. One of us (O.M.B.) was partially supported by the Soros Grant awarded by the American Physical Society (and by a Grant of the Ukrainian State Committee for Science and Technology). The main part of this work has been done during a stay of O.M.B. at the Ecole Normale Supérieure de Lyon and it has been completed during a visit of M.P at the Institute of Physics of Kiev. Both authors want to acknowledge a warm hospitality in these institutions.

REFERENCES

[1] Ya. Frenkel and T. Kontorova, 1938, Phys. Z. Sowietunion **13**, 1; Zh. Eksp. Teor. Fiz. **8**, 89.
[2] O.M. Braun and Yu.S. Kivshar, 1991, Phys. Rev. B **44**, 7694; O.M. Braun, O.A. Chubykalo, Yu.S. Kivshar, and L. Vázquez, 1993, Phys. Rev. B **48**, 3734.
[3] S. Aubry, 1983, Physica D **7**, 240.
[4] M. Peyrard and S. Aubry, 1983, J. Phys. C **16**, 1593.
[5] O.M. Braun and M. Peyrard, Phys. Rev. E **51**, 4999 (1995)
[6] O.M. Braun and M. Peyrard, Phys. Rev. B **51**, 17 158 (1995)